공학석사 학위논문

A Mobility model for TCAD simulation of current variation by random discrete dopant

랜덤 불연속 도펀트에 의한 전류 산포 TCAD 시뮬레이션에 적합한 이동도 모델

2017 년 8 월

서울대학교 대학원

전기정보공학부

유 호 인

A Mobility model for TCAD simulation of current variation by random discrete dopant

랜덤 불연속 도펀트에 의한 전류 산포 TCAD 시뮬레이션에 적합한 이동도 모델

지도 교수 박 영 준

이 논문을 공학석사 학위논문으로 제출함

2017 년 8 월

서울대학교 대학원

전기정보공학부

유 호 인

유호인의 공학석사 학위논문을 인준함

2017 년 8 월

위 원 장 박 병 국 (인)

부위원장 박 영 준 (인)

위 원 이 종 호 (인)

Abstract

In order to investigate the influence of drive current fluctuation by random discrete dopant (RDD) in the source/drain region using drift-diffusion (DD) solver, a new mobility model with 'mobility doping profile' is proposed considering the nonlocal effect of the Coulomb scattering.

The similar approach proposed by Sano is used to create a new impurity profile and introduce the charge smoothing parameter (r_{cs}) to match with the experimental values for the mobility vs. doping concentration. Smoothed doping profile with r_{cs} is used only for the doping dependent mobility calculation and the carrier localization by RDD is resolved using density gradient (DG) method. In summary, two input doping profiles is used to TCAD simulation; one for the impurity mobility and the other is the real RDD profile for the Poisson equation. It is interesting to notice that our mobility model for the RDD effect may capture some of the screening related physics even though r_{cs} is not exactly same as the screening length in the Brooks-Herring model.

In addition to the Coulomb mobility due to the RDD effect, mobility degradation by the normal field to the gate and parallel field should be considered. In particular,

degradation of the mobility due to the normal and parallel fields in the lightly doped (RDD) in the source and drain regions gives additional limitation in the driving current of the DRAM cell transistors. A strategy for the field dependent mobility models is rather empirical. The Lombardi model for normal field dependence and the extended Canali model for high field dependence with fitting parameters in the models were employed. The proposed model has been applied to the DRAM cell transistor of the 20 nm technology generation. The RDD effect in the drain region of the cell transistor alone gives relative standard variation in the driving current of ~3.1%.

In this thesis, the simple and efficient doping dependent mobility model is proposed. This model is expected to provide a clue of the variation reduction strategy together with the mobility boosting technique based on the material and device structure.

Keywords: DRAM cell transistor, random discrete dopants, TCAD simulation, doping dependent mobility model.

Student Number: 2015-22794

TABLE OF CONTENTS

List of Tables

List of Figures

Chapter 1. Introduction

1.1. Motivation

As the device size is rapidly scaled down, the variation of the device parameter such as threshold voltage, leakage and drain current etc. by the random discrete dopant (RDD) becomes important [1]-[9]. Contrary to the conventional MOSFET where the RDD in the channel region mainly contributes to the performance variations, the RDD fluctuation in the source/drain area can significantly influence the performance of the DRAM cell (Fig.1.1). There are two reasons for this. First, sub-40nm DRAM cell has adopted NMOS recessed channel array transistor with buried gate (BCAT) in order to mitigate the gate induced drain leakage current (GIDL) and parasitic capacitance of bit-line [10]. But, BCAT has the fabrication process of burying gate material under source/drain, which introduces a variation of the overlap region between source/drain and gate so that it makes an additional drive current fluctuation compared to the conventional MOSFET. Second, while the

source/drain area is scaled down, the doping concentration needs to be kept low in the DRAM cell in order to suppress the junction leakage and GIDL.

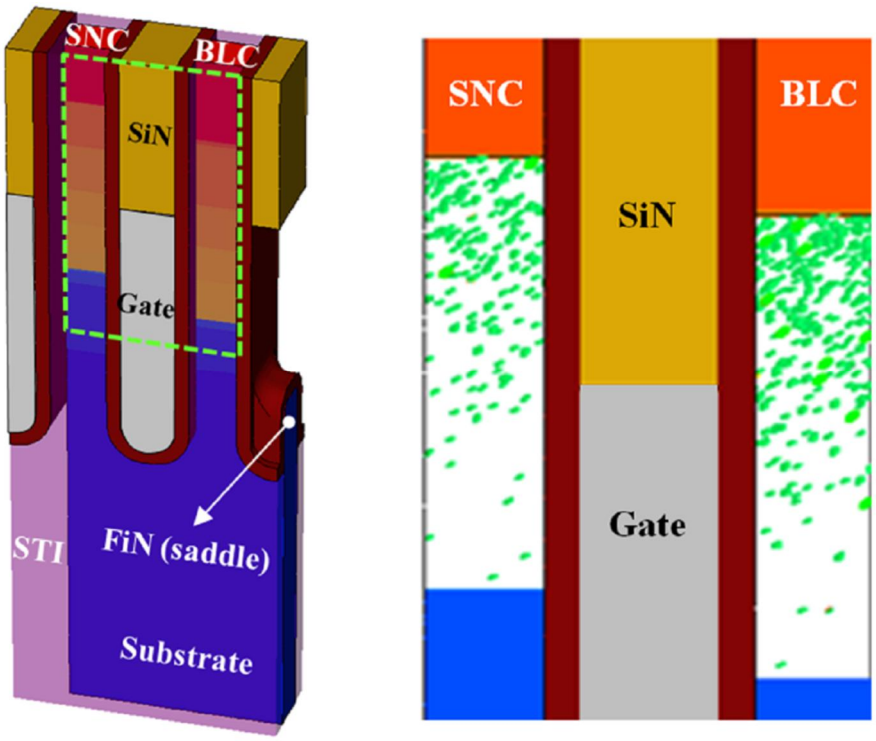

(a) (b)

Fig. 1.1 (a) Schematic view of the DRAM Cell transistor. (b) Magnified view of dashed-line in the left figure shows the discrete dopants distribution in the source/drain region of 20 nm DRAM technology generation. SNC and BLC is the abbreviation of Storage Node Contact and Bit Line Contact respectively.

Problem statement

The TCAD tools may be the only way to predict the performance of the cell transistors with the RDD before actual devices are fabricated. Two physical factors should be properly considered in the TCAD simulation; electrostatics for carrier density and the mobility. The electrostatics associated with the discrete dopants is accurately modeled by the quantum effect with density gradient (DG) method and it enables to avoid the double counting problem that occurs in splitting the Coulomb potential into short and long range components [11]-[13]. So, it has been widely applied to the study of the RDD-induced fluctuation of threshold voltage and leakage current [14], [15]. However, the Coulomb limited mobility is a nonlocal phenomenon and the mobility in the near RDD meshes cannot have the abrupt mobility differences to RDD meshes so that the doping dependent mobility model should be applied carefully when the atomistic doping profile is employed. The quasi-local mobility model based on Monte Carlo simulation results gives the accurate solution at low drain bias, but it is still unclear at high drain bias [16]. The doping dependent mobility correction method by relative error of the resistance using the atomistic resistor simulations can effectively eliminate the artifacts, but the

nonlocal effect of the Coulomb mobility has not been considered as the mobility in the meshes is still dependent on the doping of the local mesh only [17]. Even though the mobility value has been calibrated to obtain agreement between the continuous sample and the average of the RDD samples in terms of the current, the rule cannot be justified as the physical model for the RDD mobility model.

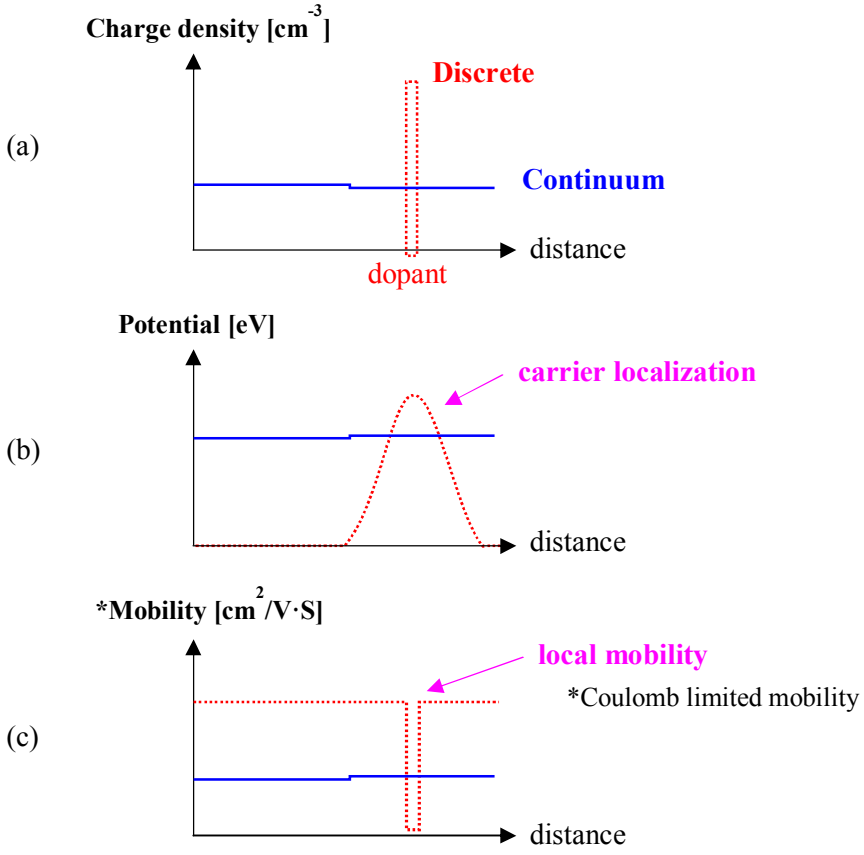

Fig. 1.2. Problems with RDD (a) are illustrated in electrostatics (b) and mobility (c).

1.2. Outline of Thesis

In this thesis, a concept of ‘mobility doping’ profile is introduced to account for the nonlocal effect of the Coulomb scattering. In this mobility doping, the doping profile is used only for the nonlocal nature of the Coulomb mobility, not for the electrostatics in solving the Poisson equation. This work does not offer a general physics-based model, but propose the correction method that can simulate the nonlocality of mobility for drift-diffusion (DD) simulations through the fitting exercises. Finally, this model is applied to the BCAT cell structure designed to meet the requirements of the 20nm DRAM technology generation [18]. The simulations are carried out with the Sentaurus tool [19] with the new RDD mobility model and used to predict the average and statistical variation of the DRAM cell current.

Chapter 2. Theoretical Background

2.1. Density gradient (DG) method

The resolution of individual charges within an atomistic simulation using a fine mesh creates problems [20]. Due to the use of Boltzmann or Fermi-Dirac statistics in classical drift-diffusion (DD) simulations the electron concentration follows the electrostatic potential, gained from the solution of the Poisson equation. As a result, a significant amount of mobile charge can become trapped (localized) in the sharply resolved Coulomb potential wells created by discrete dopant charges assigned to a fine mesh. Such trapping is physically impossible since quantum mechanical confinement keeps the ground electron state high in the well. Another effect of this charge trapping in classical simulations is the strong sensitivity of the quantity of trapped charge to the mesh size. If a finer mesh is used then the Coulomb potential well is more sharply resolved, and therefore deeper, and the amount of charge being trapped increases.

Attempts to correct these problems in atomistic simulations have been made by charge smearing or by splitting the Coulomb potential into short and long-range

components based on screening considerations [12]. In the case of charge smearing a reduction in the amount of trapping, and less mesh size sensitivity, can be achieved. This approach is however purely empirical and can result in a loss of resolution in respect to atomistic scale effects. The splitting of the Coulomb potential into short and long range components also suffers from drawbacks including the possible double counting of mobile charge screening. This method also relies upon a somewhat arbitrary cut-off point in order to separate the long and short range components.

So, in this thesis, this problem is treated quantum mechanically using DG method. The DG formalism modifies the classical electron equation of state so it contains an additional term which is dependent on the gradient of the carrier density as follows.

$$n = N_c \exp\left(\frac{E_{F,n} - E_c - \Lambda_n}{kT}\right) \qquad (1)$$

$$\Lambda_n = -\frac{\gamma\hbar^2}{6m_n^*}\frac{\nabla^2\sqrt{n}}{\sqrt{n}}$$

2.2. Mobility model

The mobility model is classified as a low electric field and a high electric field. First, the simplest case of the low field mobility is a function of the lattice temperature. This so-called constant mobility due to phonon scattering should only be used for undoped materials. For doped materials, scattering of the carriers by charged impurity ions leads to degradation of the carrier mobility, and this is so-called doping dependent mobility model. The representative models of doping dependent mobility include Masetti model, Philips unified model and ballistic model. The Masetti model [21] used in this thesis is derived to fit the experimental mobility as shown in equation (2), and most widely used model. Philips unified (Phu) model accounts for other effects such as electron–hole scattering and screening of impurities by carriers as well. The ballistic model is used for very short channel because it has been found that an additional contribution to low-field mobility is sometimes needed to match measured device characteristics. In addition, mobility degradation at interface is also included in low field mobility. In the channel region of a MOSFET, the high transverse electric field forces carriers to interact strongly

with the semiconductor–insulator interface. Carriers are subjected to scattering by acoustic surface phonons and surface roughness. In this study, the Lombardi model is used as shown in equation (3). These surface contributions to the mobility are then combined with the bulk mobility according to Matthiessen's rule (4).

In high electric fields, the carrier drift velocity is no longer proportional to the electric field, instead, the velocity saturates to a finite speed υ_{sat}. The model used in this study is Canali model [22] originates from the Caughey-Thomas [23] formula, but has temperature-dependent parameters, which were fitted up to 430K as shown in equation (5).

$$\mu_{dop} = \mu_{\min 1} \exp(-\frac{P_c}{N_{A,0} + N_{D,0}}) + \frac{\mu_{const} - \mu_{\min 2}}{1 + ((N_{A,0} + N_{D,0}) / C_r)^{\alpha}} - \frac{\mu_1}{1 + (C_s / (N_{A,0} + N_{D,0}))^{\beta}} \quad (2)$$

Parameter	Electron	Hole	Unit
μ_{min1}	52.2	44.9	cm^2/Vs
μ_{min2}	52.2	0	cm^2/Vs
μ_1	43.4	29	cm^2/Vs
P_c	0	9.23×10^{16}	cm^{-3}
C_r	9.68×10^{16}	2.23×10^{17}	cm^{-3}
C_s	3.43×10^{20}	6.10×10^{20}	cm^{-3}
α	0.68	0.719	1
β	2	2	1

Table 2.1. Parameter set for Masetti model

$$\mu_{acoustic-phonon} = \left(B\frac{T}{E_\perp} + C\frac{1}{E_\perp^{1/3}} \right)\frac{1}{T} \quad , \quad \mu_{surface-roughness} = \frac{\delta}{E_\perp^{\,2}} \qquad (3)$$

Where B is 3.1×10^8 cm/s, C is 3.0×10^7 $(V/cm)^{-2/3}\cdot$ K $\cdot$ cm/s

$$\frac{1}{\mu} = \frac{1}{\mu_{bulk}} + \frac{D}{\mu_{acoustic-phonon}} + \frac{D}{\mu_{surface-roughness}} \qquad (4)$$

Where $D = \exp(-x / l_{crit})$,

x is distance from the interface, l_{crit} is a fitting parameter

$$\mu(F) = \frac{(\alpha+1)\mu_{low}}{\alpha + \left[1 + \left(\frac{(\alpha+1)\mu_{low} F_{hfs,n}}{\upsilon_{sat}} \right)^{\beta} \right]^{1/\beta}} \qquad (5)$$

$$\beta = \beta_0 \left(\frac{T}{300K} \right)^{\beta_{\exp}} \qquad \beta_0 = 1.109 \qquad \beta_{\exp} = 0.66 \qquad \alpha = 0$$

$$\upsilon_{sat} = \upsilon_{sat,0} \left(\frac{T}{300K} \right)^{\upsilon_{sat,\exp}} \qquad \upsilon_{sat,0} = 1.07\times10^7 \qquad \upsilon_{sat,\exp} = 0.87$$

$$F_{hfs,n} = \left| \nabla \Phi_n \right|$$

Chapter 3. Simulation methodology

3.1. Sequence of mobility model development

The mobility model developments for the RDD effect use two uniformly doped resistive samples with same total dopant number; one with the continuous doping and the other samples, called the RDD samples, with uniform but random distribution of the dopants in space.

As a test structure, n-type silicon resistor of dimensions 20 nm × 20 nm × 140 nm is prepared. 100 random samples are generated with different dopant positions on intrinsic silicon for the given doping density. Discrete region length is 100nm. It is set long enough for the averaging dopants. A continuous doping region is interposed between the contacts and the discrete zone to avoid any influence related to the boundary conditions. To resolve the carrier localization by discrete dopant, the density gradient method with fine mesh is adopted. As a reference, a continuous doped resistor with the same concentration as the discrete dopant sample, hereafter the continuous sample was prepared as shown in Fig. 3.1. For the doping dependent mobility model in the low field regime, the Masetti model is employed. As for the

high-field saturation, a driving force from the gradient of the quasi-Fermi potential is adopted in order to avoid errors due to local electric field from individual dopants and use the low drain voltage to prevent the mobility degradation due to velocity saturation. The bandgap-narrowing (BGN) model is turned off. Fig. 3.2 compares the current of the resistor as a function of the doping concentration obtained from the Continuous sample and from the ensemble average of the RDD samples. When the doping-dependent mobility model is applied to the discrete doping profile without any correction, the model overestimates the current as there exist many mesh elements without any doping which has maximum constant mobility.

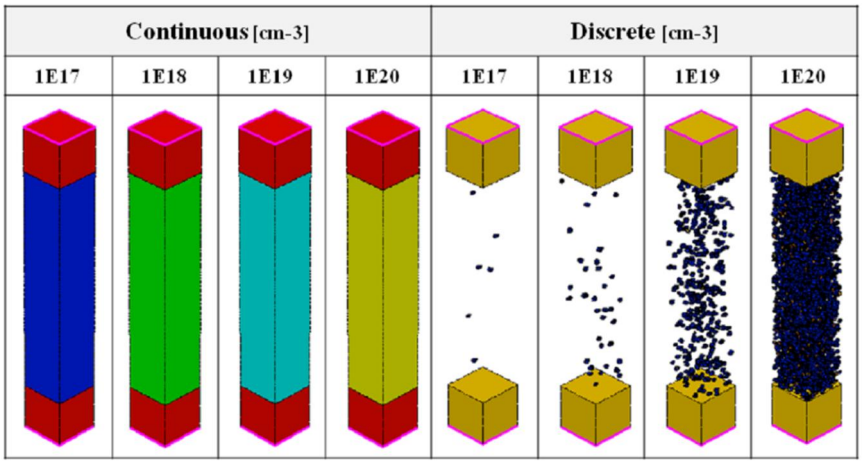

Fig. 3.1. N-type silicon resistor to compare the difference between continuous doping and discrete doping. Empty region of discrete sample is intrinsic.

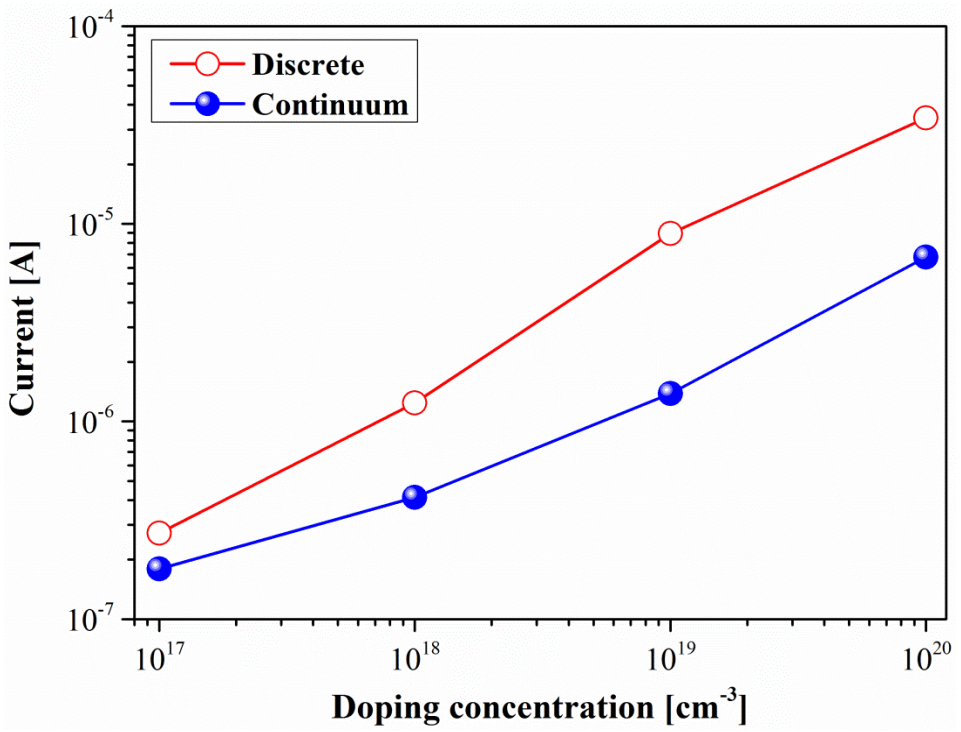

Fig. 3.2. Comparison of the current according to the doping concentration of the samples with continuous doping and discrete doping at V_D=0.02V.

3.2. Concept of the 'mobility doping'

The problem shown in Fig.3.2 is due to the local mobility as described previously. In order to include the nonlocality of the Coulomb scattering, a fictitious doping profile is introduced only for the doping dependent mobility calculation. These doping profiles are created by smoothing the atomistic doping generated on the intrinsic silicon. Although the charge created in this way cannot accurately reflect the electron trajectory around the RDD [16], this concept is roughly similar to the Rutherford scattering, where the electron is affected within a certain range from the dopant. The similar approach proposed by Sano which deals with the unphysical carrier trapping by the short range potential created by RDD is used [12]. In the approach, the Coulomb potential created by the RDD has been decomposed and the short range potential has been neglected, resulting in the corresponding charge density as follows.

$$\rho_{\text{long}}(r) = qn(r) = \frac{qk_c^3}{2\pi^2}\frac{\sin(k_c r) - (k_c r)\cos(k_c r)}{(k_c r)^3} \cdot N_f \qquad (6)$$

where k_c is the cut-off parameter for the separation of short and long range potentials, r is the radial distance from RDD, and N_f is a normalization factor such that the integral of $n(r)$ over the entire simulation space becomes unity. This charge density of the RDD is depicted according to $k_c r$ in Fig. 3.3.

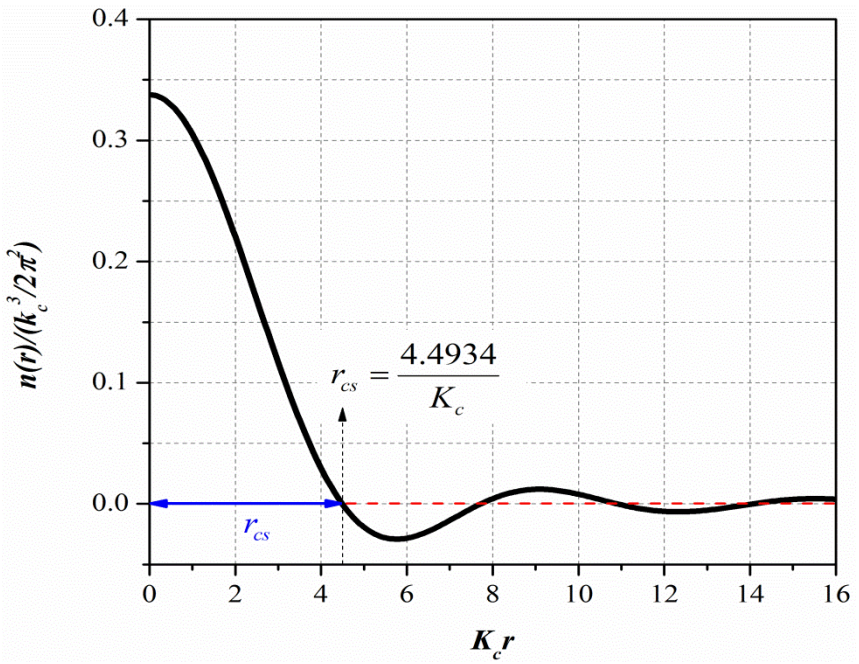

Fig. 3.3. Normalized number density of the long range part of Coulomb potential by RDD is plotted according to the parameterized radial distance. Definition of the charge smoothing radius (r_{cs}) is presented.

This function is oscillatory and becomes negative for certain values of $k_c r$, but only take the positive values before the first zero because the smoothing process of a single dopant with the specific charge is done. Since the range of the perturbation potential by the impurity, RDD in our case, is determined by the screening length in the models such as the Conwell-Weisskopf and Brooks-Herring [24], the parameter k_c can be extended to create a new impurity profile only to determine the mobility due to ionized impurity scattering. Now determination of k_c (or equivalently r_{cs} in the Fig. 3.3) in our model is not arbitrary, but to match with the experimental values for the mobility vs. doping concentration.

In summary, the parameter r_{cs} is used to account for the nonlocality of Coulomb scattering by the RDD. The determination and its physical reasoning are discussed in the following section.

3.3. The charge smoothing radius (r_{cs}) in the 'mobility doping'

In order to resolve the previously described problems, the smoothed doping with r_{cs}, keeping the position of the RDD is introduced, to reproduce the current of continuous sample. Since the number of intrinsic meshes is reduced as the charge is smoothed, the current of the RDD samples can reproduce the current of the continuous samples. These fitting exercises are carried out for a wide range doping concentration and temperatures. As a result, charge smoothing radius according to the doping concentration at various temperatures is obtained as shown in Fig. 3.4.

From this, the relationship between doping concentration and r_{cs} can be fitted by a polynomial regression as shown in the equation (7).

$$r_{cs}(x) = Ax^3 + Bx^2 + Cx + D \qquad (7)$$

where $x = \log_{10}(N_D)$, and A, B, C, and D are given in table 2. r_{cs} is used as a new fitting parameter for the Masetti doping dependent mobility correction.

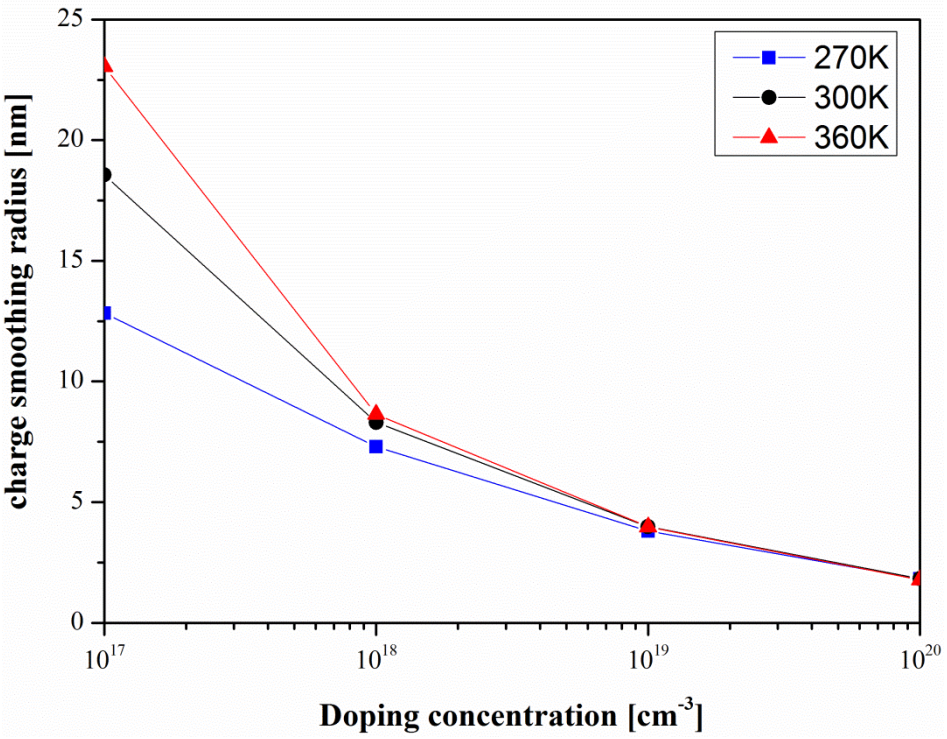

Fig. 3.4. Charge smoothing radius vs. doping concentration for three different temperatures. The charge smoothing radius is extracted by smoothing the atomistic doping of discrete samples until a continuous doping current is reproduced at each doping concentration and temperature.

	270K	300K	360K
A	-0.09202618	-0.6243197	-1.210983
B	5.998059	36.67965	70.26172
C	-130.9038	-720.2999	-1360.668
D	956.8887	4730.53	8798.33

Table 3.1. Constant values according to the temperature

Now let us consider the physical meaning of the calibrated r_{cs} in the impurity scattering. The calibrated r_{cs} values vs. doping concentration were plotted for three different temperatures. As shown in Fig. 3.4, the charge smoothing radius increases with increases in temperature and decreases in doping concentration below 10^{18} cm^{-3}. This phenomenon may be understood by the behavior of the screening length of the impurity atom by carriers. Shown in Fig. 3.5 is the screening length of the Brooks-Herring (B-H) model for various temperatures. It is interesting to notice that our mobility model for the RDD effect may capture some of the screening related physics even though r_{cs} is not exactly same as the screening length in the B-H model.

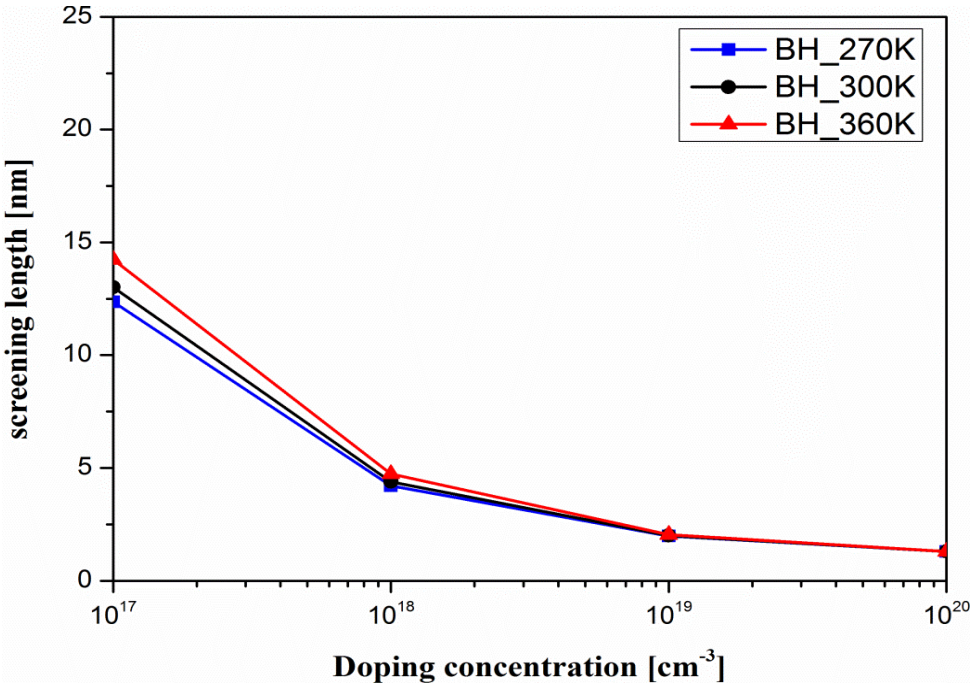

Fig. 3.5. Screening length of the Brooks-Herring as the function of doping concentration for three different temperatures.

In summary, the aim of this work is to propose the mobility correction method when the atomistic doping is employed in DD simulation. The atomistic average current is calibrated to reproduce the continuous doping current which is usually calibrated in experimental data. More specifically, the fictitious doping profile, say the mobility doping, is introduced using the r_{cs} parameter to fit the mobility with

equivalent continuous doping simulation. Finally, two input profiles are used; one for the impurity mobility and the other is the real RDD profile for the Poisson equation as shown in Fig. 3.6. Since the doping dependent mobility is calculated once in the simulation for a fixed temperature, the numerical burden is negligible.

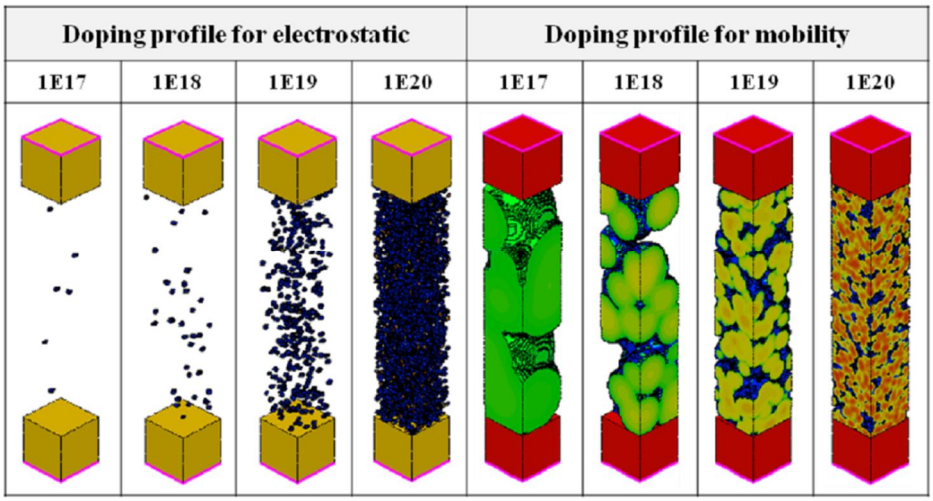

Fig. 3.6. Doping profiles as the input to TCAD simulation for the electrostatic potential and mobility. Mobility doping is obtained from electrostatic doping using charge smoothing parameter (r_{cs}). Decrease of r_{cs} is observed with increasing doping concentration.

3.4. Normal and parallel fields dependent mobility

In addition to the Coulomb mobility due to the RDD effect, mobility degradation by the normal field to the gate and parallel field should be considered. In particular, degradation of the mobility due to the normal and parallel fields in the lightly doped (RDD) in the source and drain regions gives additional limitation in the driving current of the DRAM cell transistors. In order to understand the field profiles due to the RDD effect, as shown in Fig. 3.7, two sets of simple N+NN+ bars with gate are considered, one with continuous doping and other with RDD doping.

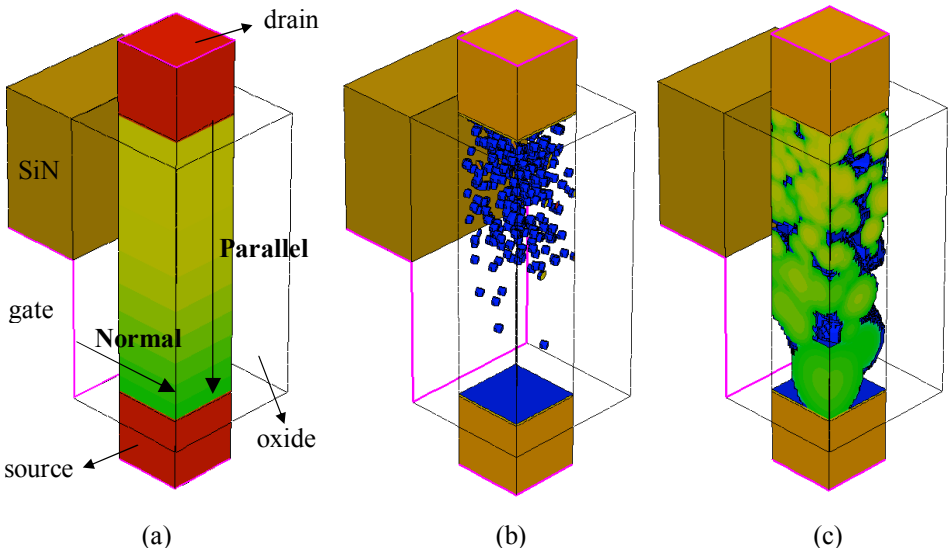

Fig. 3.7. Continuous (a) and RDD sample for electrostatics (b) and mobility (c).

The samples simulate the source/drain regions and the dimension is 20 nm × 20 nm × 80 nm. The normal and parallel electric fields in two samples are shown in Fig. 3.8. It should be noted that the field intensity for both the normal and parallel directions is different from the continuous doping case, which is the expected results of the RDD effect. The Electric field fluctuation shown in Fig.3.8 induces an additional current degradation as shown in Fig. 3.9. Our strategy for the field dependent mobility models is rather empirical. The Lombardi model for normal field dependence and the extended Canali model for parallel field dependence are employed. The fitting parameters are calibrated for the RDD sample to have the sample current as the continuous doped samples. In this procedure, first, the normal field dependent mobility is calibrated at low drain voltage and high gate voltage, and then the parallel field dependent mobility is calibrated at high drain voltage and high gate voltage. In the present case, l_{crit} in the Lombardi model and β_0 in the Canali model are the fitted to 7×10^{-7} cm and 1.7, respectively. After calibration, I-V characteristics between two samples have a good agreement as shown in Fig. 3.10.

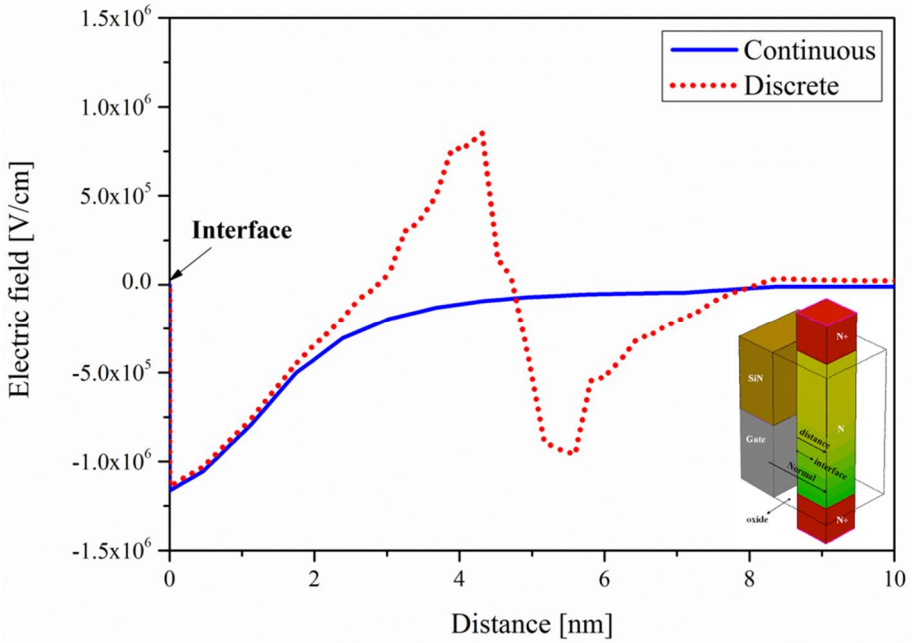
Continuous
Discrete
Interface
Electric field [V/cm]
1.5x10^6
1.0x10^6
5.0x10^5
0.0
-5.0x10^5
-1.0x10^6
-1.5x10^6
0
2
4
6
8
10
Distance [nm]
N+
SiN
Gate
N
distance
interface
Normal
oxide
N+

(a)

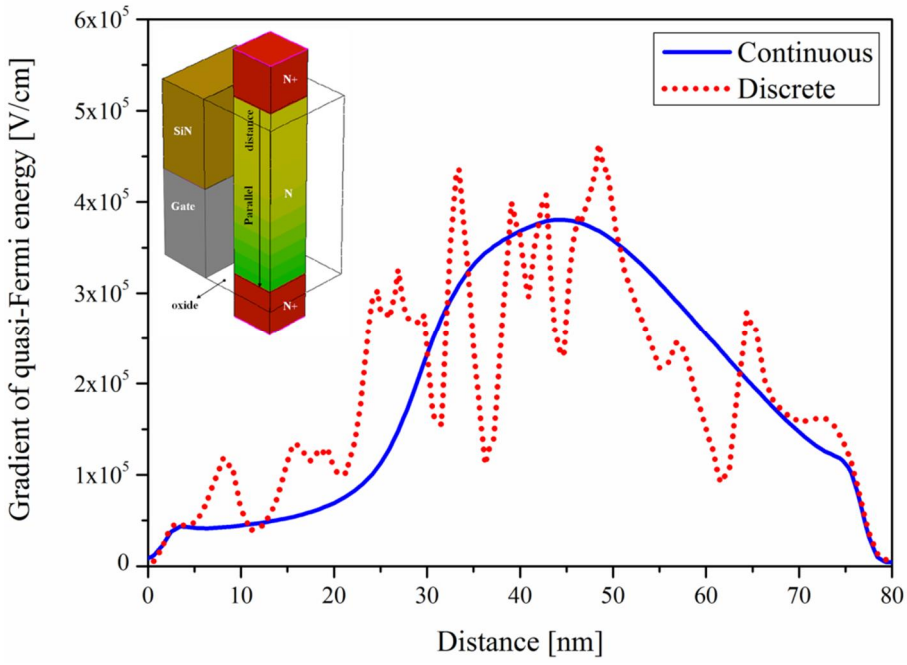
Continuous
Discrete
Gradient of quasi-Fermi energy [V/cm]
6x10^5
5x10^5
4x10^5
3x10^5
2x10^5
1x10^5
0
0
10
20
30
40
50
60
70
80
Distance [nm]
N+
SiN
distance
Gate
Parallel
N
oxide
N+

(b)

Fig. 3.8. Comparison of the (a) Normal field at V_G = 3.0V, and (b) parallel field at V_D = 1.5V with continuous doping and discrete doping.

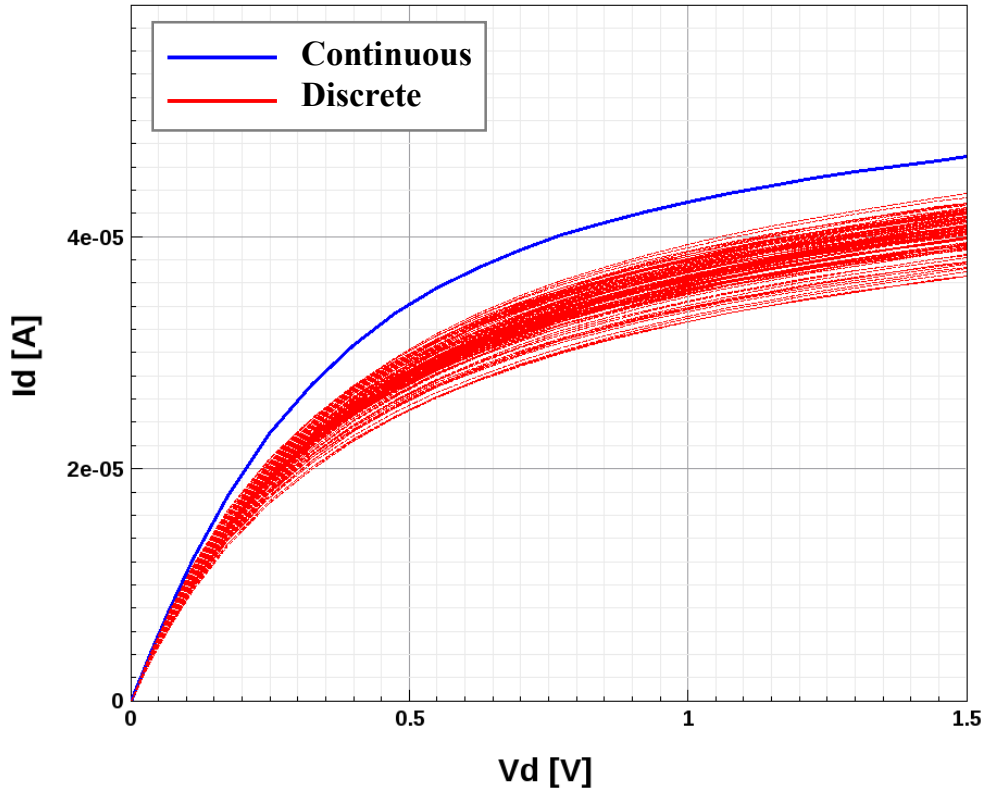

Fig. 3.9. Comparison of the I-V characteristics before calibration between continuous sample and discrete sample at V_G = 3.0V, V_D = 1.5V.

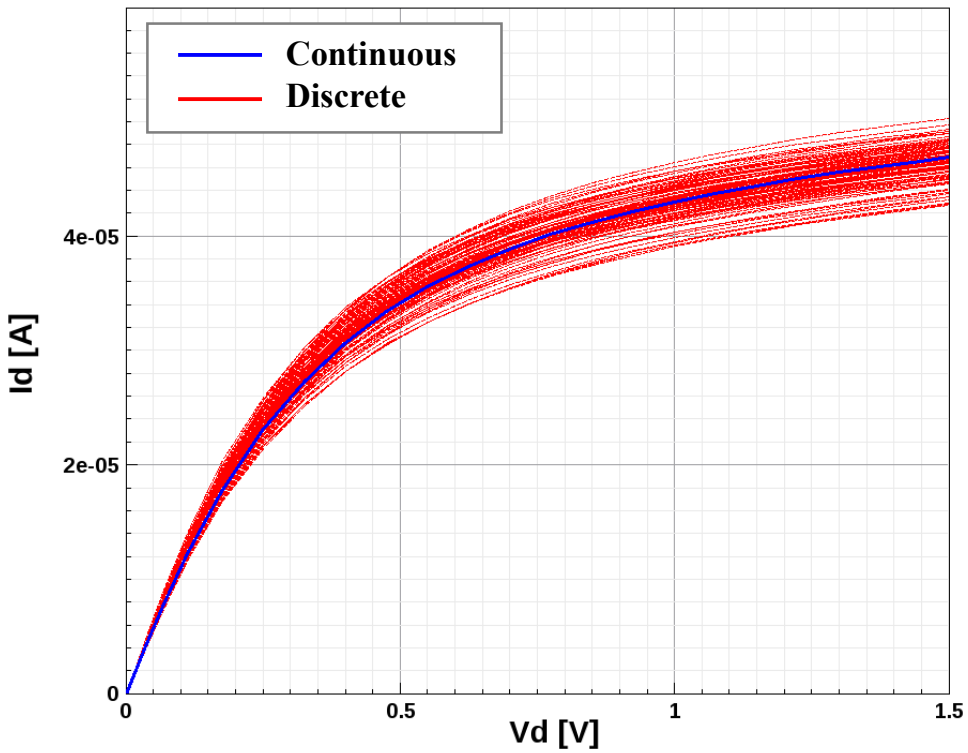

Fig. 3.10. Comparison of the I-V characteristics after calibration between continuous sample and discrete sample. l_{crit} in the Lombardi model and β_0 in the Canali model are used 7×10^{-7} cm and 1.7, respectively.

Chapter 4. Application to DRAM cell transistor

4.1. DRAM cell structure

The test devices considered in this work is a NMOS transistor with recessed channel, buried metal gate and saddle type fin. It is a structure that Samsung has used in 20 nm technology and is expected to shrink in the next generation. The design of this structure is described in detail in [18]. It has a recessed channel depth of 150 nm, critical dimension of 35 nm, fin height of 30 nm, physical gate oxide thickness of 6 nm, and buried gate is located 65 nm from the silicon surface. Gate material is TiN with the mid-gap workfunction. In order to check the influence only from the RDD at source/drain region, a continuous channel doping profile is employed. The storage and bit-line node have a dimension of 20 nm × 20 nm with asymmetric doping profiles, which are designed to satisfy requirements of driving current and the retention time characteristics. Average doping of the storage and bit-line node regions are 7×10^{18} cm^{-3}, 1.1×10^{19} cm^{-3} respectively. As shown in Fig. 4.1, the test structure has three gates to consider the neighbor cells in the array. The middle one of Fig. 4.1 (a) is the access gate (AG) and the others are pass gate (PG).

When the DRAM cell operates, positive voltage is applied to the AG and zero or negative voltage is applied to the PG. Fig. 4.1 (c) is the 'mobility doping' created from the RDD doping according to the mobility model explained in the chapter 3.3.

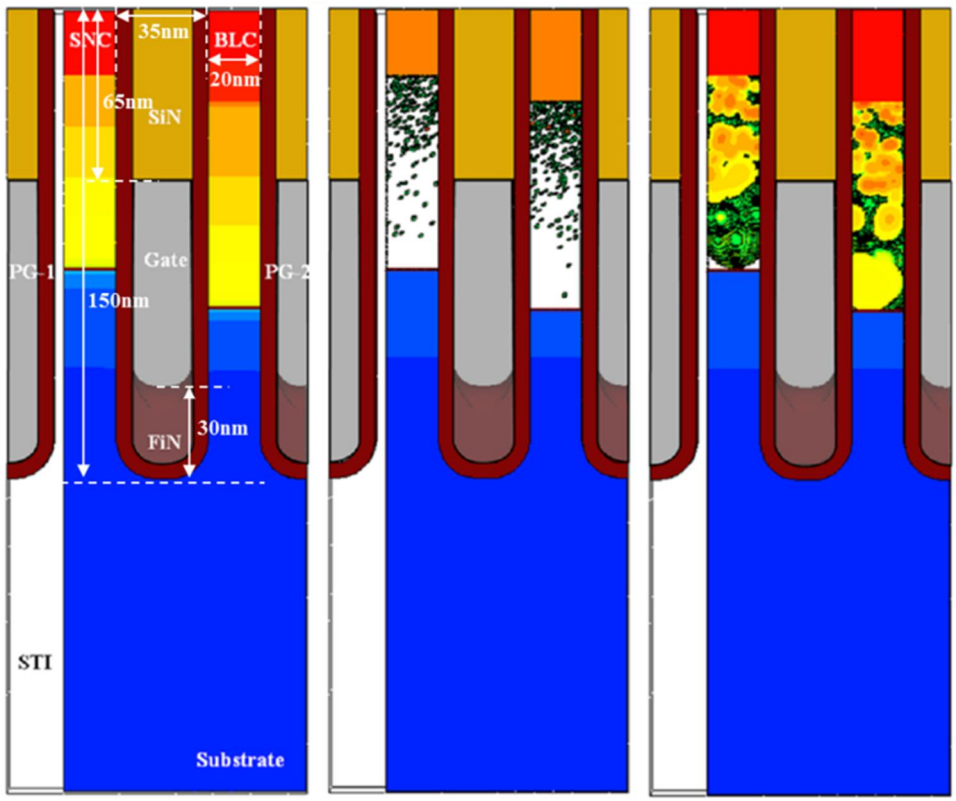

Fig. 4.1. Simulation structure and doping profile is presented. PG is an abbreviation of Pass Gate. From (a) continuous doping profile, (b) atomistic doping profile for electrostatic and (c) corrected doping profile for mobility are produced.

4.2. Impact of RDD on drive current variation

The corrected mobility model presented in the previous section to study the impact of RDD on the drive current variation is applied to DRAM cell transistor. In order to confirm our proposed model, the results between the continuous doping sample and RDD samples with original and the corrected model were compared. Since the continuous doping simulation is usually calibrated to the experimental data, this strategy is effective. The plot of the I_D-V_G transfer characteristics for atomistic doping and continuous doping at high drain bias is illustrated in Fig. 4.2. The result shows that the atomistic simulation with corrected mobility model is consistent with the continuous simulation in all regions and drive current variation by RDD is estimated the relative standard variation of 3.1%. The proposed mobility model extends the capability of the TCAD framework to predict the variation of the current drivability of DRAM cell transistors caused by the RDD effects, which become more important as the DRAM cell transistors are further scaled down.

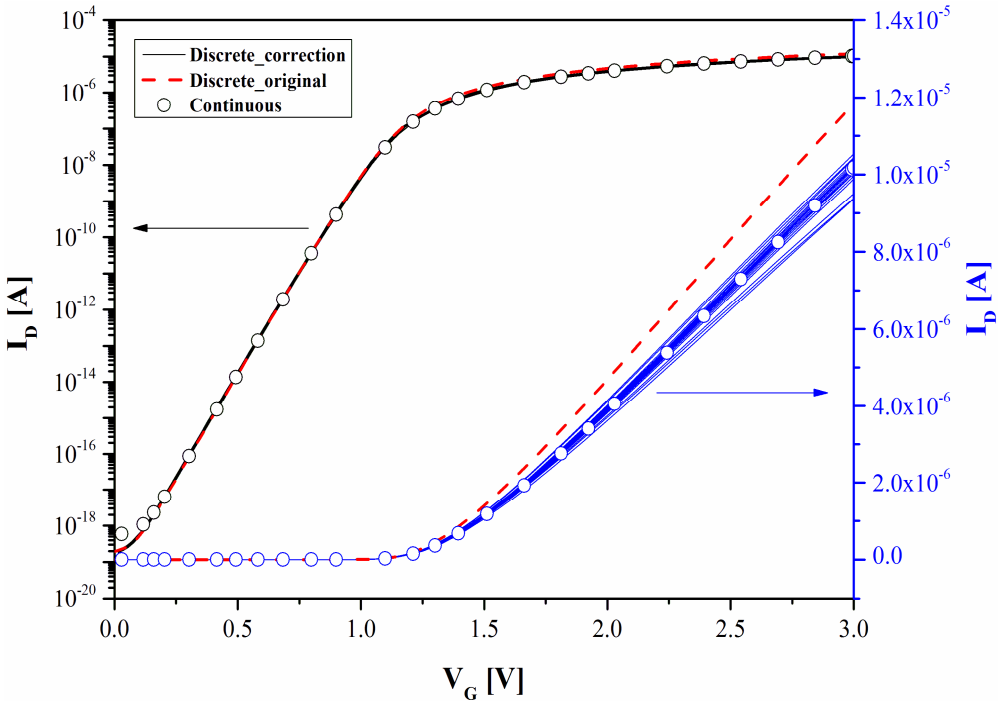

Fig. 4.2. I_D-V_G characteristics at high drain bias. Plot is drawn with logarithmic (left Y-axis) and linear scale (right Y-axis).

Chapter 5. Conclusion

In this thesis, a new 'impurity doping profile' strategy to account for nonlocality of the impurity scattering is proposed. By using the model, the influence of drive current fluctuation by RDD in the source/drain region of DRAM cell is investigated considering quantum potential by RDD. It was presented that the proposed smoothed doping can reproduce the current of continuous sample by capturing some of the screening related physics. As the average value of the DRAM cell drive current will decrease gradually as the device size is scaled down, the variation of the current due to the RDD effect becomes more important. Using the TCAD tool including our mobility model, it is expected that the reduction strategy of the variation may be found together with the mobility boosting technique based on the material and device structure [25].

Bibliography

[1] R. W. Keyes, "The effect of randomness in the distribution of impurity atoms on FET thresholds," Appl. Phys, vol. 8, pp. 251–259, 1975

[2] T. Mizuno, J.-I. Okamura, and A. Toriumi, "Experimental study of threshold voltage fluctuation due to statistical variation of channel dopant number in MOSFET's," IEEE Trans. Electron Devices, vol. 41, pp. 2216–2221, 1994.

[3] T. Mizuno "Influence of statistical spatial-nonuniformity of dopant atoms on threshold voltage in a system of many MOSFET's," Jpn. J. Appl. Phys., vol. 35, pp. 842–848, 1996.

[4] X. Tang, V. K. De, and J. D. Meindl, "Intrinsic MOSFET parameter fluctuations due to random dopant placement", IEEE Trans. VLSI System, vol. 5, no. 4, pp. 369-376, Dec.

[5] A. Asenov, "Random dopant induced threshold voltage lowering and fluctuations in sub-0.1 μm MOSFET's: A 3-D 'atomistic' simulation study," IEEE Trans. Electron Devices, vol. 45, no. 12, pp. 2505–2513, Dec. 1998.

[6] G. Roy, A. R. Brown, F. Adamu-Lema, S. Roy, and A. Asenov, "Simulation study of individual and combined sources of intrinsic parameter fluctuations in conventional nano-MOSFETs," IEEE Trans. Electron Devices, vol. 53, no. 12, pp. 3063–3070, Dec. 2006.

[7] X. Wang, A. R. Brown, N. Idris, S. Markov, G. Roy, and A. Asenov, "Statistical threshold-voltage variability in scaled decananometer bulk HKMG MOSFETs: A full-scale 3-D simulation scaling study," IEEE Trans. Electron Devices, vol. 58, no. 8, pp. 2293–2301, Aug. 2011.

[8] C. Alexander, G. Roy, and A. Asenov, "Random-dopant-induced drain current variation in Nano-MOSFETs: A three-dimensional self-consistent Monte Carlo simulation study using 'ab initio' ionized impurity scattering," IEEE Trans. Electron Devices, vol. 55, no. 11, pp. 3251–3258, Nov. 2008.

[9] S. Markov, S. Roy, and A. Asenov, "Direct tunnelling gate leakage variability in nano-CMOS transistors," IEEE Trans. Electron Devices, vol. 57, no. 11, pp. 3106–3114, Nov. 2010.

[10] K. Kim, "From the future Si technology perspective: Challenges and opportunities", Tech. Dig. IEDM, 1-9 .2010.

[11] A. Asenov, S. M. Amoroso "Problems with the continuous doping TCAD simulations of decananometer CMOS Transistors", IEEE Trans. Electron Devices, VOL. 61, NO. 8, 2014.

[12] N. Sano, K. Matsuzawa, M. Mukai, and N. Nakayama, "On discrete random dopant modeling in drift-diffusion simulations: Physical meaning of 'atomistic' dopants", Microelectron. Reliab., vol. 42, no. 2, pp. 189–199, Feb. 2002.

[13] T. Ezaki, T. Ikezawa, M. Hane, "Investigation of realistic dopant fluctuation induced device characteristics variation for Sub-100 nm CMOS by using atomic 3-D process/device simulator", IEDM Tech. Dig., pp. 311-314, 2002.

[14] G. Roy, A.R. Brown, A. Asenov, "Quantum Aspects of Resolving Discrete Charges in 'Atomistic' Device Simulations", Journal of Computational Electronics 2: 323–327, 2003.

[15] A. R. Brown, J. R. Watling, G. Roy, C. Riddet, C. L. Alexander, U. Kovac, A. Martinez, A. Asenov, "Use of density gradient quantum corrections in the simulation of statistical variability in MOSFETs", J. Comput. Electron., vol. 9, no. 3/4, pp. 187-196, Dec. 2010.

[16] S. M. Amoroso, L. Gerrer, M. Nedjalkov, R. Hussin, C. Alexander and A. Asenov, "Modeling Carrier Mobility in Nano-MOSFETs in the Presence of Discrete Trapped Charges: Accuracy and Issues", IEEE Trans. Electron Devices, VOL. 61, NO. 5, MAY 2014.

[17] S. M. Amoroso, A. R. Brown, A. Asenov, "A Mobility Correction Approach for Overcoming Artifacts in Atomistic Drift-Diffusion Simulation of Nano-MOSFETs". IEEE Trans. Electron Devices, VOL. 62, NO. 6, JUNE 2015.

[18] J. M. Park, Y. S. Hwang, S. W. Kim, S. Y. Han, J. S. Park et al., "20nm DRAM: A new beginning of another revolution", IEDM, pp. 677-679, 2015.

[19] Sentaurus TCAD Tools. Synopsys, 2015.

[20] T. Ezaki, T. Ikezawa, A. Notsu, K. Tanaka, M. Hane, "3D MOSFET simulation considering long-range Coulomb potential effects for analyzing statistical dopant-induced fluctuations associated with atomistic process simulator", Proc. SISPAD, 91, 2002.

[21] G. Masetti, M. Severi, and S. Solmi, "Modeling of carrier mobility against carrier concentration in arsenic-, phosphorus-, and boron-doped silicon," IEEE Trans. Electron Devices, vol. 30, no. 7, pp. 764–769, Jul. 1983.

[22] C. Canali, G.Majni, R. Minder and G.Ottaviani, "Electron and Hole Drift Velocity Measurements in Silicon and Their Empirical Relation to Electric Field and Temperature," IEEE Transactions on Electron Devices, vol. ED-22, no. 11, pp. 1045–1047, 1975.

[23] A. Shenk, Advanced Physical Models for Silicon Device Simulation. New York, NY, USA: Springer-Verlag, pp. 51–65, 1998.

[24] D. Chattopadhyay , H. J. Queisser, "Electron scattering by ionized impurities in semiconductors", American Physical Society, pp.749-751, 1981.

[25] K. Kim, U-In Chung, Y. W. Park, J.Y. Lee, J.H. Yeo and D.C. Kim, "Extending the DRAM and FLASH memory technologies to 10nm and beyond", Proceeding to the SPIE Advanced Lithography Conference, San Jose, Ca., February 2012.

초록

본 연구에서는 Drift-Diffusion (DD) solver를 이용하여 MOSFET 소자의 source/drain 영역에서의 random discrete dopant (RDD) 가 구동 전류의 산포에 미치는 영향을 확인하기 위해 쿨롱 산란 (Coulomb scattering) 의 비 국부적 (nonlocal) 성질을 고려하여 새로운 이동도 (mobility) 모델을 제안하였다.

새로운 모델을 만들기 위해 Sano가 제안한 전하 평활화 (charge smoothing) 방법과 유사한 접근법을 사용하여 새로운 doping profile을 생성하였고, 이를 위해 실리콘 resistor에서의 continuous 시료와 discrete 시료 간의 doping 농도별 전류 실험값을 일치시킬 수 있는 Charge smoothing radius (r_{cs})라는 parameter를 새롭게 도입하였다. r_{cs} 를 이용하여 smoothing 된 새로운 doping profile은 impurity 의존성 이동도 계산에만 사용되며, RDD에 의한 carrier localization은 quantum corrected potential을 이용한 density gradient (DG) 방법을 이용하여 해결하였다. 요약하면, RDD에 의한 TCAD simulation을 위해 기존에는 1종류의 doping profile을 사용하지만, 본 연구에서는 2종류의 doping profile을 입력하여 사용하게 되는데, 평활화된 doping profile은 impurity 의존성 mobility 계산에만 적용되고, 다른 하나는 Poisson 방정식을 풀기 위해 discrete 한 상태 그대로의 doping profile을 사용하게 된다.

여기서 드러나는 한 가지 흥미로운 사실은 앞서 도입한 r_{cs}가 실험적으로 추출한 parameter 임에도 불구하고, Brooks-Herring 모델의 screening length와 정확히 일치하진 않지만, 온도와 농도에 따른 그 경향이 유사하게 나타나는 점인데, 이로 미루어 r_{cs} 는 screening length와 연관된 Physics를 이미 내포하고 있다는 사실을 유추할 수 있다.

위의 모델을 실제 MOSFET 소자에 적용하여 전류 산포를 확인하기 위해서는 채널 표면 및 source/drain 내부에서의 전기장(electric field)에 의존하는 이동도 문제가 추가로 해결되어야 하는데, 이 부분은 Lombardi 모델과 Canali 모델을 각각 적용한 후 해당 모델에서 제공하는 fitting parameter를 이용하여 처리하였다.

이렇게 마련된 3가지 이동도 모델을 20nm급 DRAM cell transistor 구조에 적용하여 구동 전류 산포를 확인한 결과 source/drain의 RDD는 3% 수준의 구동 전류 산포를 유발하는 것으로 확인되었다.

본 연구는 기존 연구들에서 고려하지 못했던 이동도의 비 국부성(nonlocality) 을 고려하면서도 간단하고 효율적인 새로운 모델을 제안하였고, 향후 미세소자에서의 전류 boosting 기술과 함께 산포 감소 기술에 대한 전략을 제공해 줄 것으로 기대한다.

주요어: DRAM cell transistor, random discrete dopants, TCAD simulation, doping dependent mobility model

학번: 2015-22794